Electronic structure of a heterostructure of an alkylsiloxane self-assembled monolayer on silicon

D. Vuillaume,* C. Boulas, J. Collet, G. Allan, and C. Delerue
Institut d'Electronique et de Micro-Électronique du Nord, Department of Physics (isen), Boîte Postale 69, Avenue Poincaré, F-59652 Cedex, Villeneuve d'Ascq, France
(Received 17 March 1998)

We report on the experimental and theoretical determination of the energy offsets between a silicon substrate and a monolayer of alkyl chains chemically grafted on it (self-assembly technique). Internal photoemission experiments show that energy offsets between the silicon conduction band and the lowest unoccupied molecular orbital are 4.1–4.3 eV. Similarly, the energy offsets between the silicon valence band and the highest occupied molecular orbital of the alkyl chains are 4.1–4.5 eV, irrespective of the alkyl chain length (from 12 to 18 carbon atoms). These results are confirmed by theoretical calculations (the local-density approximation and tight-binding methods). These rather similar values are explained by the fact that the carbon sp_3 level tends to align with the silicon sp_3 level to achieve the charge neutrality and that the band structures of the carbon and silicon are almost centered on their respective sp_3 level. These results validate the proposed concept making use of these self-assembled monolayers as ultrathin insulator in nanometer-scale electronic devices [C. Boulas *et al.*, Phys. Rev. Lett. **76**, 4797 (1997); D. Vuillaume *et al.*, Appl. Phys. Lett. **69**, 1646 (1997)]. [S0163-1829(98)03648-0]

I. INTRODUCTION

The development and understanding of the electronic properties of organic insulating films with thicknesses in the nanometer range (say, <3 nm) are two key issues for the future of molecular nanotechnologies and molecular electronics. We have recently reported that self-assembled monolayers (SAM's) of alkyltrichlorosilane molecules chemically grafted on silicon substrate can act as very efficient insulating barriers provided their fabrication and their molecular architecture are well controlled.[1] Leakage currents through these SAM's embedded in metal-insulator-silicon heterostructures are very low (10^{-8}–10^{-7} A/cm^2 or, equivalently, a dc conductivity in the range 10^{-15}–10^{-14} S/cm) irrespective of the SAM thickness in the range 1.9–2.6 nm. This is due to tunneling energy barriers in the 4–4.5 eV range, a value so high that carrier tunneling though these ultrathin insulators is put at a nonmeasurable and negligible level.[1] These high tunneling barriers arise from the large band gap expected for these alkyl-based materials. In this paper we report on detailed experiments (internal photoemission) in order to determine the electronic structure of the metal(Al)/SAM/silicon heterostructures, i.e., the energy offset between the silicon conduction band (CB) and the lowest unoccupied molecular orbital (LUMO) of the molecular monolayer and the energy offset between the silicon valence band (VB) and the highest occupied molecular orbital (HOMO) of the molecular monolayer. This is done as a function of the length (number of carbon atoms) of the alkyl chains, i.e., as a function of the SAM thickness. These results are compared with theoretical calculations (local-density approximation and tight binding). Experiment and theory are in close agreement; they confirm and extend our preliminary results that tunneling energy barriers are very high, slightly dependent on the alkyl chain length. These energy barriers are 4.1–4.3 and 4.1–4.5 eV, for electrons and holes, respectively. The HOMO-LUMO gap of the SAM's slightly increases when decreasing the number of carbon atoms from 9.3 to 9.9 eV (18–12 atoms). The energy barriers for electrons and holes are of the same magnitude. This is due to two factors: (i) the carbon sp_3 level tends to be aligned with the silicon sp_3 level to achieve the charge neutrality and (ii) the band structures of the carbon and silicon are almost centered on their respective sp_3 level.

II. EXPERIMENTS

A. Sample preparation

The SAM's of a series of *n*-alkyltrichlorosilanes [CH_3-$(CH_2)_n$-$SiCl_3$] were chemisorbed on a solid substrate by the retraction method from solution introduced by Bigelow, Pickett, and Zisman[2] and later developed by Maoz and Sagiv.[3] As the solid substrate we used silicon wafers covered by its native oxide, since such an oxide surface is hydroxyl rich, a condition that is mandatory for a good silanization (i.e., the chemical grafting of the alkyltrichlorosilane molecules). The substrates were degenerated (resistivity of 10^{-3} Ω cm) to avoid any band bending in the substrate during electrical measurements. The thickness of the native oxide was measured [by ellipsometry and x-ray photoelectron spectroscopy[4] (XPS)] in the range 1–1.2 nm for all the substrates used during the course of this work. The thickness calculations by XPS were performed taking a value of 3.8 $\pm$0.4 nm for the electron escape depth in SiO_2 and comparing the Si_{2p} peak intensities for SiO_2 and pure silicon.[5] The native oxide surface provides a dense array ($\sim 5 \times 10^{14}$ cm^{-2}) of reactive hydroxyl groups (OH), which are the natural grafting sites for the alkyltrichlorosilane molecules dissolved at low concentrations (10^{-2}–10^{-3} M) in an inert organic solvent. In order to analyze monolayers with different thicknesses, we have used reagents with different chain lengths: *n*-dodecyltrichlorosilane (DTS), $CH_3(CH_2)_{11}SiCl_3$; *n*-hexadecyltrichlorosilane (HTS),

0163-1829/98/58(24)/16491(8)/$15.00 PRB 58 ©1998 The American Physical Society

$CH_3(CH_2)_{15}SiCl_3$; and *n*-octadecyltrichlorosilane (OTS), $CH_3(CH_2)_{17}SiCl_3$. The solvents, series of *n*-alkanes from hexane to hexadecane, were dried with molecular sieves prior to use. We used carbon tetrachloride (30% by volume) as cosolvent to help in solubilizing the polar $SiCl_3$ head groups. Extensive wet cleanings with organic and aqueous chemicals and dry cleanings by combining ultraviolet irradiation and ozone atmosphere were performed before starting the silanization process (i.e., the chemical grafting of trichlorosilane molecules).[6] These carefully cleaned silicon substrates were then dipped into the freshly prepared solution and the chemical reaction was allowed to proceed to completion. Typical reaction times were 60–90 min. This silanization process leads to well-ordered SAM's with the molecules in their all-trans conformation and their long chain axis oriented roughly perpendicular to the solid substrate.[7] There are two important controlling parameters to ensure good deposition. First, the temperature of the reactive bath has to be maintained below a critical temperature.[6] We deposited the OTS, HTS, and DTS at 14 °C, 10 °C and 2 °C, while the corresponding critical temperatures (T_C) are 29 °C, 24 °C, and 7 °C (± 3 °C), respectively. Second, the substrate to be covered has to be prehydrated with a molecularly thin layer of water.[8] The role of this surface water is twofold: (i) It allows the transformation of chlorosilane head groups ($-SiCl_3$) into trisilanol groups [$-Si(OH)_3$] by hydrolysis and (ii) it provides a fluid substrate for the molecules, which gradually adsorb on the silicon wafer, and allows them to rearrange laterally in the plane of the monolayer. This last step is necessary to form a dense, homogeneous, adsorbed layer of molecules. Once this dense layer is formed, the molecules can subsequently react to form in-plane cross links by condensation of neighboring SiOH groups into siloxane Si-O-Si linkages and with the hydroxyl groups of the solid substrate to form covalent bonds of the type *R*-Si-O-Si [where *R* is the $-(CH_2)_nCH_3$ chain]. The final state of the SAM's is a dense plane of extended hydrocarbon chains chemically linked into a two-dimensional network and grafted to the solid substrate at a certain number of hydroxyl sites (which has yet to be determined).

The critical surface tension[9] γ_c of the silane-treated surfaces were found to be $\gamma_c = 20.5 \pm 0.5$ mN/m, consistent with a top layer of methyl ($-CH_3$) groups, as it should be if the alkyl chains are densely packed. Ellipsometry[4] shows that the films were composed of a single monolayer with thickness $d = 2.65$, 2.1, and 1.83 (± 0.25) nm for the OTS, HTS, and DTS chains, respectively. In the calculation of the SAM thickness, we have used a value of 1.50 for the SAM refractive index at 633 nm.[10,7] The optical function of the oxidized substrate has been independently determined by measuring a bare wafer cleaned by rigorously the same surface cleaning process. Such values are in good agreement with the formula $d(C_n) = 0.126(n-1) + 0.478$ nm, where n is the number of carbon atoms in the alkyl chain (here 12–18), valid for hydrocarbon chains oriented perpendicular to the solid substrate and extended in their all-trans conformation.[11] The chain packing order within the monolayer is best revealed by the infrared peak positions corresponding to symmetric d^+ and antisymmetric d^- stretching of the methylene ($-CH_2$) groups. On similar OTS monolayers rigorously made according to the same process as in the present study, they are[7] at $\nu_s = 2849-2850$ cm^{-1} and $\nu_a = 2916-2918$ cm^{-1}, respectively, close to the values measured on alkane crystals but far below the positions for liquid alkanes, which are at 2856 and 2928 cm^{-1}, respectively.[7] In the present study, we measured Fourier transform infrared spectra using the attenuated total reflection (ATR) mode[12] and we found similar values ($\nu_a = 2918 \pm 1$ cm^{-1} and $\nu_s = 2850 \pm 1$ cm^{-1}) for our SAM's. We have also checked by XPS that the cleaning process does not affect the oxide layer, which is therefore always present, with the same thickness, as a sublayer below the SAM.

We fabricated the metal/SAM/silicon (MSS) structures by evaporating aluminum (100×100 μm^2, 10–100 nm thick) counterelectrodes (aluminum or gold) directly onto the SAM's through a shadow mask under ultrahigh vacuum (10^{-8} Torr). To cause the least damage to the organic layers, a low deposition rate (5–8 Å/s) was selected. We have checked that these SAM's sustain this vacuum without damage. The heating of the sample during the evaporation was also moderate enough (less than about 50 °C) so it did not create damage to the alkylsilane molecules. A thermal stability up to 350 °C (under inert ambient) has been reported for these organic films.[13] As we have reported elsewhere,[14] reasonably good capacitance-voltage characteristics are obtained for such MSS structures with interface states density of the order of 10^{11} cm^{-2} eV^{-1} and insulator charges lower than 10^{10} cm^2, despite the use of a native oxide to graft the organic molecules onto the substrate. These organic monolayers can also sustain electric fields as high as 9–12 MV/cm before breakdown.[1]

B. Internal photoemission experiments

Based on the pioneering work of Powell,[15] internal photoemission (IPE) experiments at variable excitation wavelengths allow the measurements of the energy barrier heights at both interfaces with metal and silicon. The IPE measurements were performed under monochromatic light excitation. Experiments were performed with a 150-W xenon lamp and an ORIEL monochromator working in the range 200–800 nm (~1.5–6 eV). The light beam was chopped at 3–5 Hz to allow the use of lock-in detection, which brings the photocurrent detection sensitivity down to a few 10^{-15} A. A small negative voltage (-100 to -500 mV) was applied to the metal electrode to photo-inject electrons from the metal over the energy barrier at the metal/SAM interface. On the contrary, a small positive bias (100–500 mV) was used to photoinject electrons from the degenerated *n*-type silicon. The light beam was passed through a beam splitter and the incident flux was simultaneously measured by a calibrated photodiode.

Typical photoconductivity curves are shown in Fig. 1 (Fig. 2) for the OTS, HTS, and DTS SAM's with positive (negative) bias applied on the aluminium electrode. In the first case (Fig. 1), the photocurrents are due to electrons injected from the silicon CB into the LUMO of the organic SAM over the energy barrier height Δ_e between the silicon CB and the LUMO (Δ_e is the CB/LUMO offset). According to Powell,[15] above the photoinjection threshold, linear variations are expected when plotting the cubic root of the photoresponse (the photocurrent normalized to the incident pho-

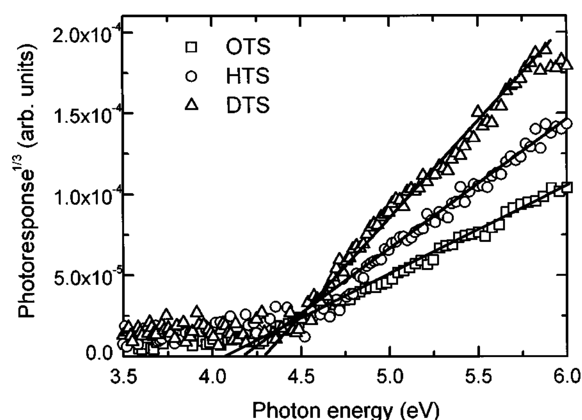

FIG. 1. Cubic root of the photoresponse (photocurrent divided by the photon flux) versus the photon energy for three OTS, HTS, and DTS monolayers. A positive bias (100–500 mV) is applied on the metal counterelectrode to photoinjected electrons from the silicon conduction band.

ton flux). In the second case (Fig. 2), the photocurrents are due either to electrons injected from the Fermi level (E_{Fm}) of the metal, provided the photon energy is higher than Δ_m the energy barrier between the metal Fermi energy and the LUMO of the molecules, or to holes injected from the degenerated silicon, provided the photon energy is higher than $\Delta_h + E_G$, E_G being the silicon band gap and Δ_h the energy barrier height between the silicon VB and the HOMO of molecules (the VB/HOMO offset).[1] In that case, above threshold, a linear variation is expected when plotting the square root of the photoresponse.[15] The values of these different thresholds can be derived from the intercepts of the extrapolated photoresponse with the photon energy x axis. In Fig. 1 we obtain $\Delta_e = 4.1 \pm 0.15$, 4.2 ± 0.15, and 4.3 ± 0.15 eV for the OTS, HTS, and DTS monolayers, respectively. Similarly, in Fig. 2 two successive thresholds (arrows A and B in Fig. 2) are clearly observed for the OTS monolayers, the first one at 4.3 ± 0.15 eV and the second one at

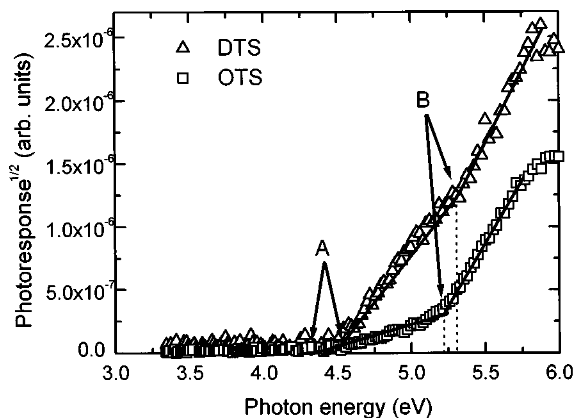

FIG. 2. Square root of the photoresponse (photocurrent divided by the photon flux) versus the photon energy for the OTS and DTS monolayers. Negative bias (-100 to -500 mV) is applied on the metal counterelectrode, electrons are photoinjected from the metal, and holes are photoinjected from the silicon substrate. Arrows A indicate the energy threshold Δ_m that electrons are to overcome to be injected in the monolayer and arrows B indicate the energy threshold $\Delta_h + E_G$ for hole photoinjection.

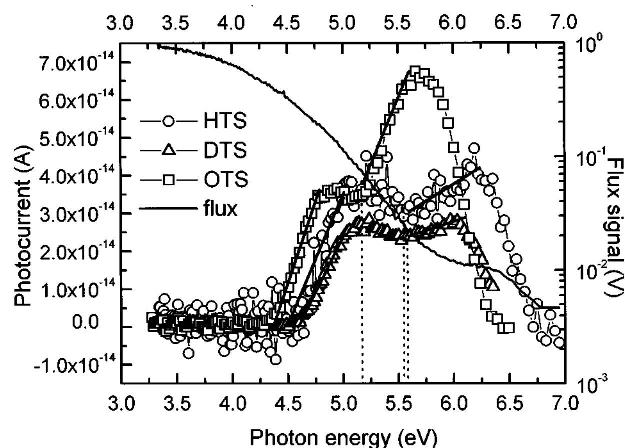

FIG. 3. Raw data of the photocurrents versus photon energy for the OTS, HTS, and DTS monolayers under negative bias applied on the metal counterelectrode. The full line is a typical photon flux measured by a calibrated photodiode for a HTS sample (similarly shaped curves apply for OTS and DTS with small measure to measure variations in amplitude depending on the optical bench alignment).

5.2 ± 0.15 eV. From the known electron affinities of the Al ($\Phi_m = 4.3$ eV) and Si electrodes ($\Phi_m = 4.05$ eV),[16] we know that Δ_m and Δ_e must differ by about 0.25 eV and thus the lowest threshold of 4.3 eV can be unambiguously attributed to Δ_m and the 5.2-eV threshold to $\Delta_h + E_G$ and then Δ_h is 4.1 ± 0.15 eV for the OTS monolayer. For the HTS and DTS monolayers, the two thresholds are less visible (only the DTS monolayer is shown in Fig. 2 for clarity). However, they are more distinguishable on the raw photocurrents (Fig. 3) as a second hump on the curves at photon energies higher than 5 eV. We ascribe these second humps to additional photocurrents over a barrier highest in energy because the photocurrents increase while the photon flux received by the sample decreases (Fig. 3). We have never observed such a second hump in the raw photocurrent curves when injecting electrons from the silicon CB. The lowest thresholds Δ_e are at 4.5 ± 0.15 eV and the highest ones are at 5.6 ± 0.15 eV for both HTS and DTS monolayers. Thus we deduce that Δ_h is 4.5 ± 0.15 eV in both HTS and DTS cases. Notice that for the OTS monolayer, the values deduced from the raw data in Fig. 3 ($\Delta_m \sim 4.3$ eV and $\Delta_h + E_G \sim 5.2$ eV) are in good agreement with those determined from Fig. 2 using the ''normalized'' data. Thus we can be confident of the values given for HTS and DTS from the raw data. All the measured values are summarized in Table I. The reason for which the hole contribution at energy higher than 5 eV is smaller in DTS and HTS monolayers (and thus less visible in the normalized data in Fig. 2) than in the OTS one is not clear.

From all these energy barrier heights, we can easily determine the HOMO-LUMO gap of the SAM of alkyl chains. It is equal to $\Delta_e + \Delta_h + E_G$. Using the above results for Δ_e and Δ_h, one obtains a value in the range 9.3–9.9 eV (± 0.3 eV) for the OTS, HTS, and DTS monolayers (Table I). We have carefully checked that these results are independent of the nature of the metal electrode. For gold, $\Phi_m = 5.1$ eV and we have indeed observed that Δ_m is shifted accordingly to 4.7–4.9 (± 0.15) eV (Fig. 4), while Δ_e and Δ_h are not affected.

TABLE I. Internal photoemission determination of the energy barriers for electrons at the Al/SAM interface (Δ_m) and Si/SAM interface (Δ_e) and for holes at the Si/SAM interface (Δ_h). The HOMO-LUMO gap of the alkyl SAM's is calculated according to $\Delta_e+\Delta_h+$silicon band gap (1.1 eV).

Monolayer	Δ_m (eV)	Δ_e (eV)	Δ_h (eV)	HOMO-LUMO gap (eV)
OTS	4.3±0.15	4.1±0.15	4.1±0.15	9.3±0.3
HTS	4.5±0.15	4.2±0.15	4.5±0.15	9.8±0.3
DTS	4.5±0.15	4.3±0.15	4.5±0.15	9.9±0.3

Since the SAM's are deposited on top of an ~1-nm-thick SiO_2 oxide layer, it is legitimate to ask to what extent this inorganic layer affects our measurements. The role of this oxide is primordial to provide an hydroxyl-rich surface that is mandatory for a successful chemical grafting of the *n*-alkyltrichlorosilane as explained in Sec. II A. Literature quotes the Si/SiO_2 interface barrier to be around 3.2 eV for thicknesses above 3 nm (Ref. 16) and even smaller for thinner layers.[17] Using electron-energy-loss spectroscopy (EELS), we showed that the gap of the ultrathin native oxide (~1 nm) on our silicon wafers is about 7 eV (Ref. 18) and thus the barrier heights are reduced accordingly. Such values are smaller than the tunneling barrier heights measured in the present experiments. The energy offset Δ at the interface obeys a transitive law $\Delta_{\text{Si-SAM}}=\Delta_{\text{Si-SiO}_2}+\Delta_{\text{SiO}_2\text{-SAM}}$ (see Sec. III for more details) and since the IPE technique measures the highest energy barrier in the heterostructure, the Si/SiO_2 energy barrier is not detected here. The same argument applies for aluminum oxide between the SAM and the top aluminum electrode. This oxide may eventually be formed after metallization when the samples are exposed to air. The energy offset between the Fermi energy of Al and the conduction band of aluminum oxide (Al_2O_3) is about 1.1 eV,[19] again much lower than the energy barrier height involved in our samples. Indeed, our IPE experiments with gold counterelectrode (*vide supra*) and thus without this oxide showed similar results.

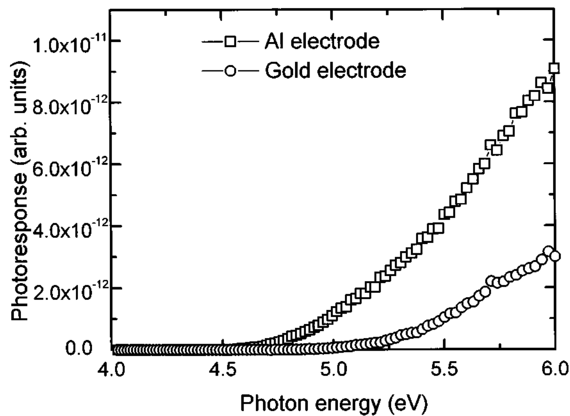

FIG. 4. Photoresponse (the photocurrent normalized to the photon flux) for two HTS monolayers, one with an aluminum counterelectrode and one with a gold counterelectrode. In both cases, a negative bias is applied on the metal electrode and the threshold corresponds to the energy barrier Δ_m.

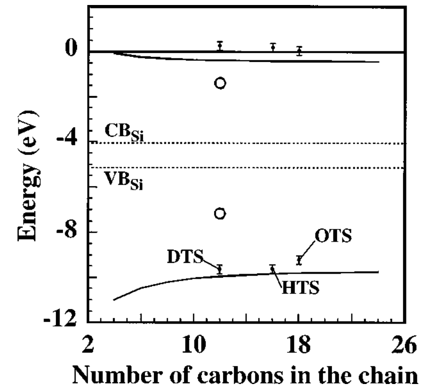

FIG. 5. Energy diagram of the silicon/alkyltrichlorosilane SAM heterostructure as a function of the alkyl chain length. Closed circles are the LUMO and HOMO levels of the OTS, HTS, and DTS SAM's measured by IPE. Solid lines are the calculated (tight-binding) LUMO and HOMO levels. Open circles are the LUMO and HOMO levels for a chain of 12 carbon atoms calculated by the LDA. Dotted lines are the experimental values of the silicon CB and VB.

So, if we neglect the native oxide (see the theoretical justification in Sec. III), the energetic band diagram of the MSS structure deduced from our IPE measurements is schematically shown in Fig. 5. Irrespective of the chain length (here between 12 and 18 carbon atoms), the LUMO band lies around at the vacuum level, a result in agreement with the known electronic structure of bulk polyethylene.[20] However, the HOMO-LUMO gaps we have measured for monolayers are slightly higher than those measured in bulk polyethylene (~8.8 eV).[20] From our experiments, we get that the HOMO band of the alkyl monolayers lies about 5.2–5.6 eV below the Fermi energy of the semiconductor (assuming that the Fermi energy lines up the bottom of the conduction band in the degenerated silicon) and thus about 9.3–9.9 eV below the vacuum level. All these results are also in close agreement with previously reported data on quite similar alkyl chains deposited on solids by the Langmuir-Blodgett technique. Ueno *et al.*[21] reporting on UV photoemission spectroscopy on Langmuir-Blodgett films of cadmium salt of arachidic acid and Segi *et al.*[22] for n-$C_{86}H_{74}$ films have found the HOMO level at about 10 eV below the vacuum level.

III. THEORY

The electronic structure of the polyethylene chain $(CH_2)_n$ has been previously calculated by various methods including semiempirical and *ab initio* methods.[23] On bulk polyethylene, HOMO-LUMO gaps from 9.6 to 19.5 eV and positive electron affinities from 0.3 to 7 eV have been reported (see the quoted values in Ref. 20). From a careful analysis of these results, it is found that the position of the HOMO is quite constant over all of these calculations, −9.9 to −13.3 eV (quite constant, at least compared to the scattering of the calculated HOMO-LUMO gap). *Ab initio* calculations for an infinite chains by Karpfen[23] show the HOMO at about 10 eV below the vacuum energy level (at momentum $k=0$) in good agreement with the results of the angle-resolved photoemission experiments using synchrotron radiation reported by Ueno *et al.*[21] and Segi *et al.*[22] Recent calculations using

the density-functional theory give HOMO-LUMO gaps of 7.7–8 eV (Ref. 24) and 5.7–6 eV.[25]

In this work we focused on a different topic, namely, the calculation of the band offsets at the interface between the silicon and the alkyl chains and on the variations of these band offsets as a function of the chain length (from 4 to 24 carbon atoms). We cannot simply use the previous calculations on bulk material to validate the present experiments for a monolayer chemisorbed on a semiconductor because when the *n*-alkyltrichlorosilanes are chemisorbed, a charge transfer occurs between the adsorbed molecules and the silicon substrate (or the oxide layer) that induces electrostatic potential variations. Thus a new self-consistent calculation of the electronic structure of the whole structure must be done. This has been performed using two methods: one based on the density-functional theory within the local-density approximation (LDA) and one based on the tight-binding technique. The former one is *ab initio* but is computer time consuming. For insulators, it also suffers from the well-known problem of an underestimation of the band gap.[26] For the computation, we used the DSOLID code[27] where the electronic wave functions are developed in a basis of atomic orbitals. We used a double numeric basis set (two atomic orbitals for each occupied orbital in the free atom) together with polarization functions ($3d$ for Si and O and $2p$ for H) and the spin-density functional of Vosko, Wilk, and Nusair.[28] All the states are calculated self-consistently with respect to the charge density and the potential (including core states, which will be useful to determine the band offsets). The tight-binding technique is semiempirical. It has already been applied with success to semiconductor heterojunctions.[29] An sp_3s^* atomic basis is used to describe the silicon and carbon atoms and one s orbital for each hydrogen atom. The terms of the Hamiltonian matrix are restricted to the intra-atomic terms and to the interactions between nearest-neighbor atoms. We take the parameters of Robertson[30] for Si-Si, Si-O, and C-C interactions. The C-H interactions ($ss\sigma$ and $sp\sigma$ following the notations of Slater and Koster[31]) and the energy E_{H} of the hydrogen s orbital are fitted in order to get an electronic structure of the C_2H_6 molecule in tight binding in good agreement with the one obtained in the LDA (after application of a rigid shift of 4 eV of the unoccupied states with respect to the occupied states corresponding to the self-energy correction of the band gap as discussed below). We obtain $ss\sigma=-4.95$ eV, $sp\sigma=5.98$ eV, and $E_{\mathrm{H}}=-3.78$ eV.

The problem is rather similar to the calculation of the band offset at a semiconductor heterojunction and we shall use some of the results obtained for this kind of system.[29]

(i) The screening length of the charge transfer in semiconductors is of the order of one interatomic distance. So the charge transfer is localized in very few planes close to the interface.

(ii) The electrostatic potential is screened by a quantity equal to the mean value of the static dielectric constants of the two materials. This screening is very efficient in the case of a semiconductor heterojunction when both interface components have bulk values close to ~10–12. That means that the charge transfer is strongly reduced by the screening. In the case of the chemisorption of CH_2 chains on a Si or SiO_2 surface, it is more difficult to evaluate, but in any case remains larger than half the bulk silicon value (~12). This gives rise to very small charge transfers across the interface, but also between planes parallel to the interface. A good approximation often used in the tight-binding method applied to this class of problems is to approximate the self-consistent potential by its value calculated assuming that all the planes parallel to the interface remain neutral.[29] This, however, allows charge transfers between atoms in the same plane, notably between C and H atoms.

(iii) The band offset transitivity for three semiconductors A, B, and C ($\Delta E_{AB}=\Delta E_{AC}+\Delta E_{CB}$) has been verified for a large number of heterojunctions.[32] Using this result here, we can strongly simplify our calculation assuming that the $(CH_2)_n$ chains are chemisorbed on the Si atoms without any SiO_2 layer at the interface ($\Delta E_{\text{Si-(CH}_2)_n}=\Delta E_{\text{Si-SiO}_2}+\Delta E_{\text{SiO}_2\text{-(CH}_2)_n}$). This can be understood in simple terms in the zero-charge-transfer approximation applied to a sp_3 molecular model. The Si sp_3 molecular orbital must be aligned with the oxygen p level at the Si-SiO_2 interface and on the other side the oxygen p level is aligned with the carbon sp_3 one. As a first-order approximation the valence-band offset does not depend on the presence of a SiO_2 layer. Such an assumption has been verified by first principles using DSOLID:[27] Introducing an oxygen atom between the silicon surface layer and the first carbon of the $(CH_2)_n$ chains does not modify the Si-$(CH_2)_n$ band offset. Thus we do not include the SiO_2 layer in our calculations. This band offset transitivity rule is also well suitable for the band offset measurement by the IPE technique as explained in Sec. III B and the comparison between measurements and the present calculations is thus meaningful.

(iv) This last point means that the valence-band offset does not depend very much on the interface orientation and its variation between (100), (110), and (111) interfaces is quite small. For obvious technical reasons, we replace the semi-infinite silicon substrate by a slab containing 15 (110) layers of silicon atoms, which is sufficient to simulate the electronic properties of the bulk silicon. A (110) surface allows one to simply grow the $(CH_2)_n$ chains normally to the Si surface. For the LDA calculation, we assume that only one chain is chemisorbed per surface unit cell; the dangling bond of the second Si atom in the unit cell is in this case saturated by a hydrogen atom. This leads to a density of one molecule per surface of 20.8 Å^2 that compares well with the experimental situation [20–22 Å^2 (Ref. 33)]. In the tight-binding case, a $(CH_2)_n$ chain is chemisorbed on each Si surface atom, but we neglect the interactions between two neighboring chains.

The local densities of states obtained using the tight-binding method are shown in Fig. 6 for atoms close to the interface. They rapidly converge to the ''bulk'' values when one moves away from the interface. Nevertheless, it is difficult to accurately determine the barrier heights Δ_e and Δ_h from these density of states. This difficulty has been solved in the case of the LDA using the material core levels as common energy references (Fig. 7). Then one has simply to know for each separate material α (=1 or 2) the energy difference ΔE_{VC}^{α} between the top of the valence band (HOMO in the case of the molecule) and a bulk core level (here $1s$) and for the heterojunction the difference in energy

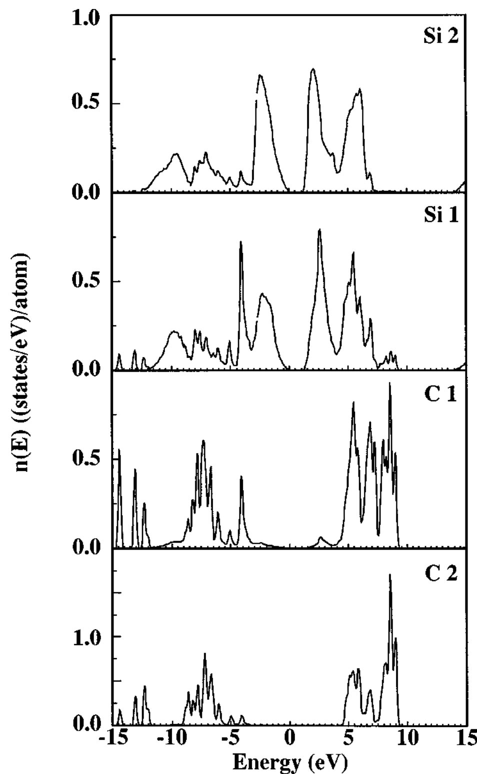

FIG. 6. Local densities of states near the Si-C interface (the atoms are labeled according to their position in relation to the interface).

ΔE_C between the two core levels. From this we easily determine Δ_h (Fig. 7).

$$\Delta_h = \Delta E_C + \Delta E_{VC}^1 - \Delta E_{VC}^2. \tag{1}$$

Such a procedure is still easier within the tight-binding and zero-charge approximations where the LDA core levels E_C^α are replaced by the self-consistent sp_3 level $E_{sp_3}^\alpha$ for each material.[34] Then the barrier height Δ_h is given by $\Delta E_{sp_3} + \Delta E_{vsp_3}^1 - \Delta E_{vsp_3}^2$, where ΔE_{sp_3} is the net energy difference between the sp_3 levels of the two materials and $\Delta E_{vsp_3}^\alpha$ is the energy difference between the top of the valence band and the sp_3 level in the material α, which is obtained from the bulk band structure. The quantities $\Delta E_{vsp_3}^1$ and $\Delta E_{vsp_3}^2$ for the bulk infinite materials and for the semi-infinite ones are equal in the case of an heterojunction. This is also true for the silicon substrate, but the molecular chain is finite and

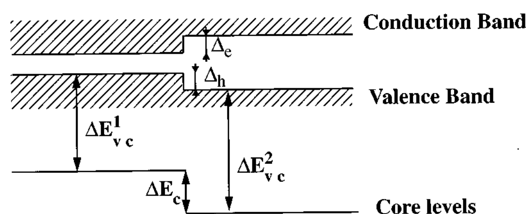

FIG. 7. Determination of the valence-band offset from core-level energies.

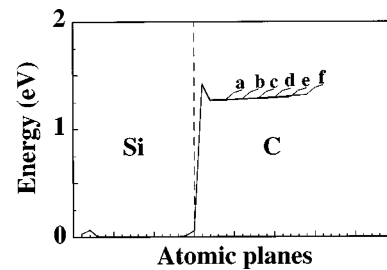

FIG. 8. Tight-binding position of the sp_3 levels in the zero-charge model. The zero energy is taken at the bulk sp_3 level. The dotted line shows the position of the Si plane close to the interface. Fifteen Si planes are used for the substrate. Curves a–f correspond to alkyl chains with 6, 8, 10, 10, and 14 C atoms, respectively.

there is a small variation of $\Delta E_{vsp_3}^{CH_2}$ between the isolated and the adsorbed molecules. We have verified that the effect of a variation of the tight-binding parameters of a hydrogen atom belonging to the CH_3 group at the end of the chain is quite small. In the following $\Delta E_{vsp_3}^{CH_2}$ is assumed to remain constant.

Let us first look at the variations of the sp_3 energy (Fig. 8). The electrostatic dipole potential at the Si-C interface does not depend on the length of the chain and its variations from a mean value are small and strongly localized near the interface. A small variation also occurs near the carbon atom at the free end of the chain. This is due to the extra C-H bond in the CH_3 group compared to a carbon atom near the middle of the chain.

We have represented in Fig. 5 the energetic band diagram calculated using the tight-binding method as a function of the number of carbon atoms in the chain. The values obtained using the LDA for a chain with 12 carbon atoms are also shown for comparison. The band gap of the molecule in the LDA (5.8 eV), in good agreement with previous calculations by the LDA [~5.7–6 eV (Ref. 25)], is much smaller than using the tight-binding method (9.55 eV) because of the band-gap problem of the LDA.[26] As the calculation of the self-energy correction $\Delta\Sigma$ to the band gap is far beyond the scope of the present paper, we have made a simple estimation using the empirical rule of Fiorentini and Baldereschi,[35] which establishes that $\Delta\Sigma$ varies like $9/\varepsilon$ in eV, where ε is the static dielectric constant of the material.[36] Using the experimental value $\varepsilon = 2.25$ for monolayers of alkyl chains,[7,10] we obtain $\Delta\Sigma = 4$ eV. Then the corrected LDA gap for a chain of 12 carbon atoms is 9.8 eV. We obtain that the gap is almost independent on the length of the molecule when the number of carbon atoms is greater than 10. The positions in energy of the HOMO and LUMO with respect to the silicon band structure are in agreement with the experimental data within 0.3 eV. We confirm that the barrier heights Δ_e and Δ_h have a similar magnitude. This is due to two factors: (i) the carbon sp_3 level tends to be aligned with the silicon sp_3 level in order to achieve the charge neutrality and (ii) the band structures of carbon and silicon are almost centered on their respective sp_3 level.

IV. CONCLUSION

Internal photoemission was used to determine the electronic structure of silicon/alkyl chain heterostructures (energy offset, HOMO-LUMO gap). High values were found for both the CB/LUMO offset (4.1–4.3 eV) and the VB/HOMO offset (4.1–4.5 eV) irrespective of the alkyl chain length (12–18 carbon atoms). These results were confirmed by theoretical calculations (the local-density approximation and the tight-binding method). Both these results validate the proposed concept to use these self-assembled monolayers as an ultrathin insulator in nanometer-scale electronic devices.[1,13,37–39]

ACKNOWLEDGMENTS

We are indebted to A. Leroy and A. Fantorini for metallization, J.-P. Nys for EELS measurements, E. Bergignat, A. Gagnaire, and G. Hollinger for XPS and ellipsometry measurements, and J. Davidovits and F. Rondelez for precious help and advice on the fabrication of self-assembled monolayers. This work was financially supported by Ultimatech-CNRS and IFCPAR (Project No. 1614-1). The ''Institut d'Electronique et de Micro-Électronique du Nord'' is ''Unité Mixte 9929 du Centre National de la Recherche Scientifique.''

*Author to whom correspondence should be addressed. Electronic address: vuillaume@isen.iemn.univ-lille1.fr

[1] (a) C. Boulas, J. V. Davidovits, F. Rondelez, and D. Vuillaume, Phys. Rev. Lett. **76**, 4797 (1997); (b) D. Vuillaume, C. Boulas, J. Collet, J. V. Davidovits, and F. Rondelez, Appl. Phys. Lett. **69**, 1646 (1997).

[2] W. C. Bigelow, D. L. Pickett, and W. A. Zisman, J. Colloid. Sci. **1**, 513 (1946).

[3] R. Maoz and J. Sagiv, J. Colloid Interface Sci. **100**, 465 (1984).

[4] E. Bergignat, A. Gagnaire, and G. Hollinger (private communication).

[5] R. Saoudi, G. Hollinger, A. Gagnaire, P. Ferret, and M. Pitival, J. Phys. III **3**, 1479 (1993).

[6] J.-B. Brzoska, N. Shahidzadeh, and F. Rondelez, Nature (London) **360**, 719 (1992); J.-B. Brzoska, I. Ben Azouz, and F. Rondelez, Langmuir **10**, 4367 (1994).

[7] A. N. Parikh, D. L. Allara, I. B. Azouz, and F. Rondelez, J. Phys. Chem. **98**, 7577 (1994).

[8] D. L. Allara, A. N. Parikh, and F. Rondelez, Langmuir **11**, 2357 (1995); D. L. Angst and G. W. Simmons, *ibid.* **7**, 2236 (1991); J. D. Le Grange, J. L. Markham, and C. R. Kurkjian, *ibid.* **9**, 1749 (1993); C. P. Tripp and M. L. Hair, *ibid.* **8**, 1120 (1992); M. E. Mc Govern, K. M. R. Kallury, and M. Thompson, *ibid.* **10**, 3607 (1994).

[9] We used the extrapolation technique of Zisman [W. A. Zisman, Adv. Chem. Ser. **43**, 1 (1964)] in which the contact angles for sessile drops of homologous apolar liquids are plotted as a function of their liquid-vapor interfacial energy γ_{LV}. To measure the contact angles, we used an optical method described in detail elsewhere (Ref. 6), in which the droplet acts as a convex mirror for a parallel light beam form a He-Ne laser, incident perpendicular to the analyzed surface. The advantage of this technique is its ability to measure low contact angles with great accuracy ($\pm 0.5°$). That allows us to use homologous series of alkanes with their γ_{LV} close to γ_C (Ref. 6). We also used a remote-computer controlled goniometer system (DIGIDROP by GBX, France) to measure water contact angles greater than 90° on silanized surfaces, values for which the above method cannot be used. Advancing and receding angles were measured using a tilted sample holder table. All measurements (both techniques) were made in ambient atmosphere and at room temperature.

[10] A. Ulman, *An Introduction to Ultrathin Organic Films: From Langmuir-Blodgett to Self-Assembly* (Academic, San Diego, 1991).

[11] S. R. Wassermam, Y. T. To, and G. M. Whitesides, Langmuir **5**, 1074 (1989).

[12] We used a Perkin-Elmer Spectrum 2000 spectrometer equipped with a Spectra-Tech 4× beam condenser (Model 0010-336) with a micro ATR holder and home-made silicon ATR crystal ($10 \times 5 \times 1.5\ \mathrm{mm}^3$, 45°), the sample chamber being purged with dry nitrogen. Spectra were recorded at 4-cm^{-1} resolution. Two hundred scans were coadded and were Fourier transformed with strong apodization. The spectra were referenced against the one obtained for the silicon ATR clean crystal before silanization.

[13] D. Vuillaume, in *Amorphous and Crystalline Insulating Thin Films*, edited by W. L. Warren, R. A. Devine, M. Matsumura, S. Cristoloveanu, Y. Homma, and J. Kanicki, MRS Symposia Proceedings No. 446 (Materials Research Society, Pittsburgh, 1997), p. 79; J. Collet, Ph.D. thesis, University of Lille, 1997.

[14] P. Fontaine, D. Goguenheim, D. Deresmes, D. Vuillaume, M. Garet, and F. Rondelez, Appl. Phys. Lett. **62**, 2256 (1993).

[15] R. J. Powell, J. Appl. Phys. **41**, 2424 (1970).

[16] S. M. Sze, *Physics of Semiconductor Devices* (Wiley, New York, 1981); E. R. Nicollian and J. R. Brews, *MOS Physics and Technology* (Wiley, New York, 1982).

[17] S. Horiguchi and H. Yoshino, J. Appl. Phys. **58**, 1597 (1985); see also Ref. 1(b) and references therein.

[18] EELS experiments were performed with a homemade system using a cylindrical mirror analysis (CMA). The samples are bombarded with a primary electrons at $E_p = 80$ eV, normal incidence, and in a standard single-pass CMA pulse counting mode. We applied an EELS procedure describe in P. Poveda and A. Glachant, Surf. Sci. **323**, 258 (1995).

[19] R. Stratton, J. Phys. Chem. Solids **23**, 1177 (1962).

[20] K. J. Less and E. G. Wilson, J. Phys. C **6**, 3110 (1973).

[21] N. Ueno, W. Gädeke, E. E. Koch, R. Engelhardt, R. Dudde, L. Laxhuber, and H. Möhwald, J. Mol. Electron. **1**, 19 (1985).

[22] K. Segi, U. Kartsson, E. Engelhardt, and E. E. Koch, Chem. Phys. Lett. **103**, 343 (1984).

[23] A. Karpfen, J. Chem. Phys. **75**, 238 (1981), and references therein for a detailed review of theoretical results. See also Ref. 20 for quoted values.

[24] M. S. Miao, P. E. van Camp, V. E. van Doren, J. J. Ladik, and J. W. Minimire, Phys. Rev. B **54**, 10 430 (1996).

[25] B. Montanari and R. O. Jones, Chem. Phys. Lett. **272**, 347 (1997).

[26] L. J. Sham and M. Schüter, Phys. Rev. Lett. **51**, 1888 (1983); J. P. Perdew and M. Levy, *ibid.* **51**, 1884 (1983).

[27] *Dsolid User Guide* (Molecular Simulations, San Diego, 1996), Version 9.7.

[28] S. J. Vosko, L. Wilk, and M. Nusair, Can. J. Phys. **58**, 1200 (1980).

[29] C. Priester, G. Allan, and M. Lannoo, Phys. Rev. B **33**, 7386 (1986).
[30] J. Robertson, Philos. Mag. B **66**, 615 (1992).
[31] J. C. Slater and G. F. Koster, Phys. Rev. **94**, 1498 (1954).
[32] See, for example, in *Heterojunction Band Discontinuities: Physics and Applications*, edited by F. Capasso and G. Margaritondo (North-Holland, New York, 1987).
[33] I. M. Tidswell, B. M. Ocko, P. S. Perghan, S. R. Wasaerman, G. M. Whitesides, and J. D. Axe, Phys. Rev. B **41**, 1111 (1990).
[34] C. Priester, G. Allan, and M. Lannoo, Phys. Rev. Lett. **58**, 1989 (1987).
[35] V. Fiorentini and A. Baldereschi, Phys. Rev. B **51**, 17 196 (1995).
[36] The empirical rule of Ref. 35 has been tested on many different systems including organic molecules such as C_{60}.
[37] J. Collet, D. Vuillaume, M. Bonnier, O. Bouloussa, and F. Rondelez, in *Electrical, Optical and Magnetic Properties of Organic Solid-State Materials IV*, edited by L. Chiang, L. Dalton, A. Jen, J. Reynolds, and M. Rubner, MRS Symposia Proceedings No. 488 (Materials Research Society, Pittsburgh, in press).
[38] J. Collet, O. Tharaud, C. Legrand, A. Chapoton, and D. Vuillaume (Ref. 37).
[39] J. Collet and D. Vuillaume, Appl. Phys. Lett. (to be published).